

## A comprehensive model for ICE oriented to the electronic control of the injection

M. Anatone, R. Carapellucci, R. Cipollone, A. Sciarretta  
Dipartimento di Energetica, University of L'Aquila  
Montelucio di Roio, 67040 L'Aquila, Italy

### Abstract

The electronic control of spark ignition port injected engines requires simulation tools able to predict online the relevant dynamics concurring to the mixture formation, mainly during engine transients.

A comprehensive mathematical model, specifically conceived for this application, is presented in this paper. The model is based on a time-dependent physically consistent description of the main processes. The most peculiar aspect is the integration between the description of the air and exhaust gas dynamics inside the manifolds and the model for the fuel dynamics in liquid and vapour phases. The gas model describes the pressure wave propagation in the ducts in a lumped-parameter way; the fuel model adopts a quasi-lagrangian two-dimensional approach for the spray and a zero-dimensional representation for the fuel puddles. The overall model, which has a modular structure, also accounts for the other relevant processes occurring in the engine, such as combustion, heat transfer, pollutants formation, shaft dynamics, etc.

The model has been applied on a one-cylinder, electronically injected, research engine (AVL 540), that is under testing by the authors. The results obtained for the air and exhaust dynamics point out the accuracy of the model when compared with the more complex and resource-consuming method of characteristics. The model has been then applied to build the steady air maps of the engine and to characterize the parameters of an universally adopted fuel dynamics model ( $X-t$ ) at different operating conditions.

### Nomenclature

$A$	<u>Latin letters</u> upstream boundary condition slope	$S$	stroke	$r$	downstream
$a$	speed of sound	$t$	time	rem	removed
$B$	downstream boundary condition slope	$U$	internal energy	$s$	upstream
$C$	characteristic curve slope	$u$	fluid velocity	$\infty$	steady state
$c$	propagation velocity	$V$	volume		<u>Acronyms</u>
$D$	diameter	$V_c$	engine displacement	AFR	air-fuel ratio
$\dot{E}$	internally generated heat flux	$X-t$	Aquino model parameters	BDC	bottom dead center
$h$	specific enthalpy		<u>Greek letters</u>	BMEVP	brake mean effective pressure
$k$	ratio of specific heats	$\lambda$	QPM model parameter	EVC	exhaust valve closing
$L$	length	$\tau$	time constant	EVO	exhaust valve opening
$m$	mass	$w$	pulsation	IVC	inlet valve closing
$N$	engine speed		<u>Superscripts</u>	IVO	inlet valve opening
$p$	pressure	(i)	referred to i-th species	MOC	method of characteristics
$\dot{Q}$	exchanged heat flux		<u>Subscripts</u>	QPM	quasi propagatory model
$r_c$	compression ratio	gen	generated	TDC	top dead center
		in	inlet	WOT	wide open throttle
		j	referred to j-th capacity		
		o	initial values		
		out	outlet		

## 1 Introduction

The need of Internal Combustion Engine (ICE) models specifically oriented to the port injection control is twofold, regarding the on-board, as well as the out-of-board applications. In the first case, the main goal is the evaluation, on the running engine, of the fuel to be injected in order to fulfil the requirements in terms of fuel economy and emission control (pollutants formation and effectiveness of the after-treatment devices), without derating the expected engine performances (driveability, power and torque, etc.) (Maki *et al.*, 1995; Ohata *et al.*, 1995; Nasu *et al.*, 1996). In the second case, the importance of the specific models is recognized in the pre-optimization stages of the air fuel ratio (AFR) control strategies, embedded in the electronic board: this should allow for an effective reduction of the time-to-market of a new application (Weeks and Moskwa, 1995; Cipollone and Sciarretta, 1998c).

In both cases, the reduction of the hardware and software resources required by the models appears strongly necessary. It is, of course, more important for the on-board application, where the engine speed fixes the time available for the control. Though compatible with the hardware and software on-board capabilities, and matching with the present-day on-board sensors, electronic conditioning etc. (Toyota Engine Technology 1996, Ch. 5), the models must be physically consistent. In out-of-board applications, the availability of fast but effective codes may be important as well, allowing for a large number of off-line optimization operations.

In this framework, the physical processes concerning the air and fuel dynamics in the intake manifolds play a dominant role. For these processes, the Mean Value Engine Models (MVEM) represent an advanced proposal, as shown in (Hendricks, 1996), appearing to have the most interesting capabilities for a model-based AFR control. Nevertheless, they present some remarkable limits: the usual engine configurations, mainly for multi-cylinder engines, are hard to be modeled in the proposed way; the use of the sole volume to describe a filling-emptying process is not satisfactorily representative of the inertial properties (dependent on the ducts length), mainly during rapidly varying transients. Moreover, the success of these models still depends on the adoption of steady state engine data (volumetric efficiency) that must be stored in the control unit. Finally the complex geometry of the intake system between the throttle valve and the intake valves, cannot be represented as a unique volume. Due to these limiting factors, a different modeling approach for the air and fuel dynamics, representing a transition towards truly instantaneous values models, should be considered.

In order to achieve a computational tool, running as a "virtual engine", in this paper a comprehensive engine model oriented to the electronic control of the port injection is presented. It has been conceived in a modular form: the description of the processes can be done according to several possibilities, characterized by a growing complexity, in order to fulfil the different requirements of on-board and out-of-board applications. A key role in this model is played by the description of the fluodynamic transient phenomena in the intake and exhaust engine manifolds. A lumped parameter approach taking into account the propagatory phenomena among the capacities (Quasi Propagatory Model – QPM) (Cipollone and Sciarretta, 1998a, 1998b) has been introduced. The dynamics of the fuel has been described in liquid and vapour phases, adopting a quasi-lagrangian two-dimensional description for the drops motion and a zero-dimensional approach for the fuel puddles (Anatone *et al.*, 1998a).

The two models have been integrated in the overall engine model, considering also the in-cylinder processes and the crank shaft dynamics. The link between the gas and fuel models is based on a limited number of parameters, with the aim to properly simplify their formulation and then to make the overall engine model eligible for online, on-board electronic control.

The model has been applied on a one-cylinder research engine (AVL 540) under testing by the authors, to characterize the dynamic interactions between air and fuel in the intake port, considering both steady and transient engine conditions.

## 2 Model description

The proposed model describes a multi-cylinder engine as a collection of *capacities*, in which the thermodynamic properties of fluids are concentrated, and transfer *branches*, through which mass and energy fluxes are exchanged between two capacities. This schematization has been selected as a valid compromise between the need to describe air, fuel and exhaust dynamics in unsteady terms, and the simplicity of a lumped-parameter structure, without involving a one-dimensional modelization (method of characteristics - finite difference or finite elements methods) for the propagation phenomena. In this way, a finite number of state variables to be used in control applications can be recognized.

For both intake and exhaust systems, the code allows to introduce any number of capacities. This is done by constructing each capacity around a section where the properties are calculated, and defining in a suitable way a volume representing the adjacent duct branches. The sketch in Figure 1 illustrates how a proper selection can be made, for a generic intake duct configuration, being one capacity and two transfer branches highlighted. An appropriate definition of the capacities allows for an effective representation for the actual configuration of the engine intake and exhaust systems, accounting for filters, throttle valves, collectors, mufflers, catalytic converters, etc.

Similarly, the cylinder can be described, according to the required modelling detail, in terms of two or more capacities. In the simpler case, the two capacities are the gas volume and the oil volume, which are

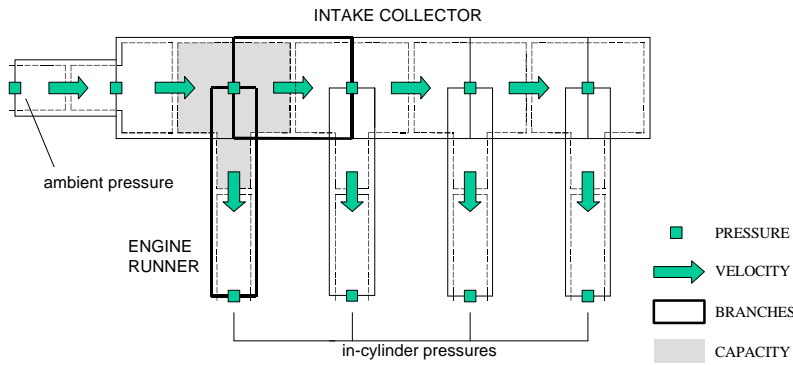


Figure 1: A generic capacity-transfer branches scheme representing a multi-cylinder intake system

variable as the piston moves. In the other cases, the in-cylinder gas capacity can be further divided in a flame front, a burned gas region, an unburned zone. Also the oil layer can be considered as a capacity having its own properties. In each capacity, the model calculates pressure and temperature, air, fuel and exhaust masses, and also the concentration of the species  $N_2$ ,  $O_2$ ,  $H_2O$ ,  $CO_2$ ,  $H_2$ , and of the in-cylinder dissociation products  $CO$ ,  $OH$ ,  $H$ ,  $O$ ,  $NO$ .

The variables describing the thermodynamic state of a capacity have been calculated according to mass and energy conservation laws, considering uniform properties within the capacity. The time variation of the mass of the generic  $i$ -th species in the  $j$ -th capacity,  $m_j^{(i)}$ , is given by:

$$\frac{dm_j^{(i)}}{dt} = \dot{m}_{j,in}^{(i)} - \dot{m}_{j,out}^{(i)} + \dot{m}_{j,gen}^{(i)} - \dot{m}_{j,rem}^{(i)} \quad (1)$$

in which  $m_{j,gen}^{(i)}$  and  $m_{j,rem}^{(i)}$  are the source and sink terms. They can be associated to liquid fuel (drops and films) evaporation, as in the intake system, or to chemical reactions, as in the cylinder and in the exhaust system.

The temperature of the  $j$ -th capacity comes from the energy conservation law in the form:

$$\frac{dU_j}{dt} = \dot{m}_{j,in} h_{j,in} - \dot{m}_{j,out} h_{j,out} + \dot{E}_j + \dot{Q}_j - p_j \frac{dV_j}{dt} \quad (2)$$

Enthalpy terms of Eq. (2) describe the energy exchanges with j-1 and j+1 capacities; the term  $\dot{E}_j$  is associated to a mass flux, while the terms  $\dot{Q}_j$  and  $p_j(dV_j/dt)$  account for thermal and work exchanges, respectively.

The key terms for a proper evaluation of Eq. (1) and (2) are represented by  $\dot{m}_{j,in}^{(i)}$  and  $\dot{m}_{j,out}^{(i)}$ , which are the mass flows between two capacities, that are evaluated as in the following section.

## 2.1 The air and exhaust gas dynamics model

The conventional lumped-parameter models, such those discussed in (Horlock and Winterbone, 1986; Heywood, 1988), calculate the mass flow  $\dot{m}$  exchanged between the j and the j+1 capacity as depending only on the instantaneous values of the thermodynamic properties upstream and downstream the flux. For engine applications, this steady approach could be unsuitable, being the time scale of the mass transfer between the capacities comparable with the upstream and downstream thermodynamic properties rate of change. Hence, the QPM, already presented in (Cipollone and Sciarretta, 1998a, 1998b), has been here adopted for a deeper description of the mass flows exchanged by the capacities. The QPM introduces, for each transfer branch - Figure 1 -, a dynamical relationship between the fluid velocity (and hence mass flow rate), at the midpoint of the branch -  $u$  -, and the boundary conditions at the ends of the branch.

These conditions express a relation between upstream and downstream pressures ( $p_s$  and  $p_r$ , respectively) and velocity, at pipe ends. The intersection of the two boundary conditions, gives the steady values of velocity  $u_\infty$  and pressure  $p_\infty$  in the branch. A correction of these values in presence of heat flows, either due to internal heat generation or thermal exchanges and friction, can be introduced as in (Cipollone and Sciarretta, 1998b).

In order to characterize the dynamic behaviour of the fluid in the branch, a transition from an initial state ( $u_0, p_0$ ) towards the equilibrium ( $u_\infty, p_\infty$ ) must be considered.

The QPM model shows that the velocity of the flow at the branch midpoint follows a first order dynamic model:

$$\frac{du}{dt} = \frac{u_\infty - u}{t_{QPM}} \quad (3)$$

for  $I > 0$ , and a second-order dynamic model:

$$\frac{d^2u}{dt^2} = -\frac{2}{t} \frac{du}{dt} + \left( \frac{1}{t_{QPM}^2} + w_{QPM}^2 \right) \cdot (u_\infty - u) \quad (4)$$

for  $I < 0$ , being  $I = [(C - B)/(C + B)] \cdot [(C - A)/(C + A)]$ , with  $A = (p_s - p_\infty)/u_\infty$ ,  $B = (p_\infty - p_r)/u_\infty$ ,  $C = \pm(kp_0/a_0)$ .

The time lag  $t_{QPM}$  and the damped pulsation  $w_{QPM}$  have the following formulations:

$$t_{QPM} = -\frac{2L}{c \ln|I|} \quad w_{QPM} = \frac{pc}{2L} \quad (5)$$

being  $L$  the branch length and  $c = u \pm a$  the absolute propagation velocity of the pressure waves (direct and reverse with respect to the stream), allowing for a finer description of the inlet and exhaust engine systems.

It must be emphasized that the known boundary conditions are – referring to Figure 1 – at the pipe inlet and at the runner outlet (in-cylinder conditions). All the other properties (velocity at the midpoint of the

branches and pressure in the capacities) can be evaluated by an iterative procedure that makes use of Eq. (3) and (4) and of the mass (1) and energy conservation (2) equations applied at the capacities.

## 2.2 The fuel model

The air and fuel mixing in the intake port is the result of a complex interaction of the fuel spray with the pulsating air flow, and of the impact on hot walls, with subsequent evaporation or formation of liquid puddles. All these aspects have been considered in a phenomenological way in the fuel model, already presented in (Anatone *et al.*, 1998a), that has been here adapted for integration with the air model. The model adopts a quasi-lagrangian, two dimensional formulation for the spray, while the fuel puddles (at the port walls and on the valve) have a zero-dimensional representation.

Table 1 reports the equations describing the most relevant phenomena which affect the drops and the films. A general scheme of the fuel paths from the injector to the cylinder is shown in Figure 2: the model can calculate the fuel mass stored in each form (film on the valve, at port wall, etc.) and the contribution of liquid and vapour to the inducted fuel mass.

The drops in the conic spray, whose size distribution has been derived from experimental results (Anatone *et al.*, 1998b), have been grouped into parcels, having the same diameter. Each parcel is injected at a random angle within the spray cone's opening, to simulate the intrinsic availability of the spray formation process. The sequence of parcels is repeated for a number of sequentially time-spaced steps, until all the fuel mass has been injected.

<p><u>Spray formation</u></p> $V_{inj} = \frac{R_e^{\frac{5}{6}}}{17.11 \frac{L_{or}}{d_{or}} + 1.65 R_e^{0.8}} \sqrt{\frac{2(p_f - p_i)}{\rho_f}}$		<p><u>Film motion</u></p> $\frac{d(m_f V_f)}{dt} = F_a - \mathbf{m}_c A_{w-f} \frac{V_f}{h_f} + m_f g \sin \mathbf{y}$ $F_a = \frac{1}{2} f A_{f-a} \rho_a V_a^2 \quad \text{film on the port wall}$ $F_a = C_{dva} A_{f-a} \frac{1}{2} \rho_a V_a^2 \quad \text{film on the valve}$			
<p><u>Droplet motion</u></p> $\frac{d(m_d \bar{V}_d)}{dt} = -C_d \frac{\rho}{4} d_d^2 \frac{1}{2} \rho_a  \bar{V}_d - \bar{V}_a  ( \bar{V}_d - \bar{V}_a )$		<p><u>Film evaporation and thermal energy exchange</u></p> $\dot{m}_{ev} = \frac{A_{w-f}}{D} D_m \rho_m S_h \ln \left( 1 + \frac{Y_v - Y_{v\infty}}{1 - Y_{vs}} \right)$			
<p><u>Drop heat exchange and evaporation</u></p> $\dot{m}_{ev} = - \frac{\dot{Q}_{a-d}}{[I - C_d(T_d - T_r)]} \quad \text{for } T_d = T_b$ $\dot{m}_{ev} = \rho d_d D_m \rho_m S_h \ln \left( 1 + \frac{Y_v - Y_{v\infty}}{1 - Y_{vs}} \right) \quad \text{for } T_d < T_b$					
$A_{f-a}$	valve wetted area	$m_{ev}$	evaporated mass flow rate	$Y_v$	fuel vapour mass fraction
$A_{w-f}$	port wall wetted area	$m_f$	film mass	$Y_{vs}$	fuel vapour mass fraction (saturation)
$C_d$	drag coefficient (drops)	$p_f$	fuel pressure	$Y_{v\mathbf{y}}$	fuel vapour mass fraction (mixture)
$C_{dva}$	drag coefficient (valve film)	$p_i$	intake pressure	$I$	latent heat
$C_{pd}$	fuel specific heat	$Q_{a-d}$	heat flow (air-drops)	$\mathbf{m}$	fuel viscosity
$D_m$	molecular diffusivity	$T_b$	fuel boiling temperature	$\rho_a$	air density
$d_{or}$	injector orifice diameter	$T_d$	drops temperature	$\rho_m$	mixture density
$F_a$	drag force on the film	$T_r$	reference temperature	$\mathbf{y}$	port angle
$f$	friction coefficient	$V_a$	air velocity		
$h_f$	film thickness	$V_d$	drops velocity		
$L_{or}$	injector orifice length	$V_f$	film velocity		
$m_d$	drops mass	$V_{inj}$	injection velocity		

Table 1: Equations for relevant fuel spray processes

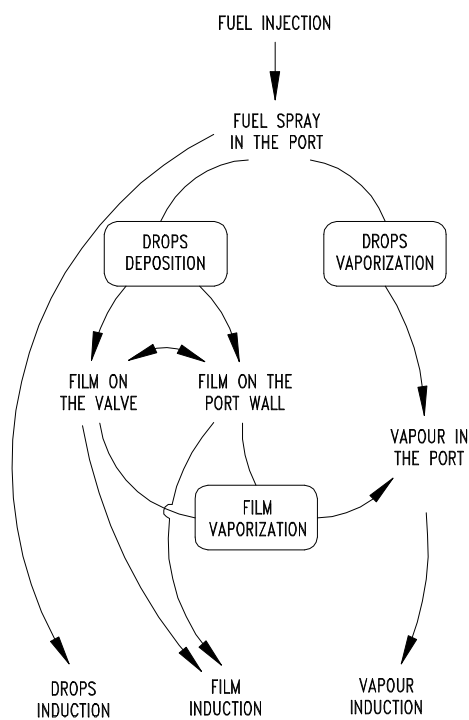


Figure 2: Fuel paths in the intake port

Starting from the initial velocity and temperature conditions, the droplets are followed in their motion, applying to each of them the momentum and energy conservation laws. The initial velocity of all particles is assumed equal to the jet velocity  $V_{inj}$ . For the droplet motion, the aerodynamic (drag and lift) forces, inertial (virtual mass and Basset) forces, volume (gravity and buoyance) forces and pressure forces have been evaluated, observing that all are negligible when compared to the drag force. In order to apply the energy equation, the drops evaporation and the thermal exchange between drops and surrounding air have been considered.

In the zero-dimensional modeling of each of the two puddles introduced, a constant film area has been assumed, and defined from geometric considerations, including the surface roughness effects. Also for the puddles, the momentum and energy equations have been applied, instead of considering steady relations often adopted in literature (Couette flow). For the port puddle motion, the air entrainment force, the viscous force between film and manifold walls, and the gravity force have been considered; for the valve puddle, the air drag force substitutes the air entrainment force. The complex thermal exchanges with the flowing air and the walls have been considered for both the puddles, together with the evaporation terms.

### 2.3 The overall model

The fuel model formulation has been properly adapted to match the requirements of the air dynamics as described by the QPM. The QPM gives to the fuel model the kinematics and thermodynamics parameters of the air, while receiving the mass (in liquid and vapour phases) and energy fuel flows. The fuel vapour inside the air stream is taken into account, assuming it as uniformly distributed within a capacity.

The engine model has been completed considering:

- a) closed volume (in-cylinder gas), described by different thermodynamic models with an increasing level of complexity (single- or multiple- zone, accounting for flame front, burned or unburned gases, oil layer etc.);
- b) heat losses, described by a lumped-parameter model accounting for the thermal resistive and capacitive properties of the engine components and their thermal interactions with the in-cylinder gas and the refrigerating fluids;
- c) mass losses in oil sump;
- d) crank shaft dynamics.

A schematic representation of the architecture of the overall engine model is reported in Figure 3, showing the main interactions among the sub-models. A great flexibility allows to add new devices or to change the level of description of the processes already present.

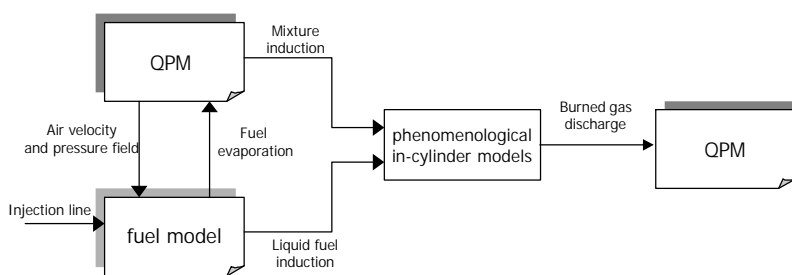


Figure 3: Overall engine model

### 3 Results

The overall model has been applied to simulate the behaviour of a one-cylinder, electronically injected, research engine (AVL 540), that is under testing by the authors. The different volumes (capacities) that define the geometry of the intake and exhaust systems are shown in Figure 4, being the values reported in Table 2. Table 3 summarizes the main engine characteristics.

The engine has been simulated considering the speed in the range 2000-5000 rpm and the load in the range 20-100%, corresponding to the throttle positions (TP) listed in Table 4.

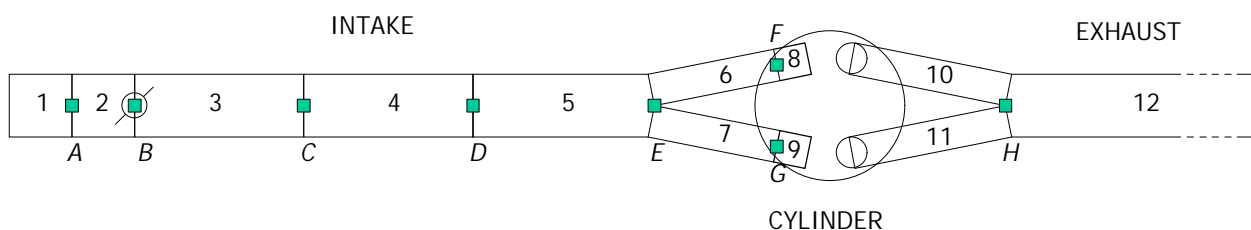


Figure 4: Simulated engine sketch (12 branches; 8 capacities)

$V_1$	50.0 cm <sup>3</sup>	$V_5$	104.1 cm <sup>3</sup>
$V_2$	91.1 cm <sup>3</sup>	$V_6$	21.6 cm <sup>3</sup>
$V_3$	131.9 cm <sup>3</sup>	$V_7$	21.6 cm <sup>3</sup>
$V_4$	131.9 cm <sup>3</sup>	$V_8$	356.4 cm <sup>3</sup>

Table 2: Volumes of the capacities in Figure 4

$V_C$	499.6 cm <sup>3</sup>	IVO	33° before TDC
$r_c$	10.5	IVC	56° past BDC
$S$	8.6 cm	EVO	73° before BDC
$D_{IV}$	2.32 cm	EVC	15° past TDC
$D_{EV}$	2.30 cm		

Table 3: Main engine characteristics

#### 3.1 Air and gas dynamics

In order to validate the model prediction, the calculated pressure and velocity values have been compared with those derived by the method of characteristics (MOC), that effectively represents the unsteadiness of the process.

In Figures 5 and 6, the fluid velocity at the midpoint of branch “8” and the pressure in capacity “E” (which includes the duct junction) - Figure 4 - are reported as a function of the crank angle. The QPM (solid line) introduces only slight errors with respect to the MOC (dashed line). In particular, the QPM appears to underestimate the back flow velocity in the early stage of the induction process, while it overestimates the maximum intake velocity; in any cases, the differences are negligible at all engine speeds and loads. The same agreement is obtained observing the pressures: the frequency of the fluctuations are still correctly estimated (Figure 6d).

Throttle Position (TP)	Engine load $\left( \frac{BMEP}{BMEP_{MAX}} \right)$
1 (WOT)	100%
2	70-75% (*)
3	45-55% (*)
4	20-25% (*)

(\*) Depending on the engine speed

Table 4: Engine operating conditions

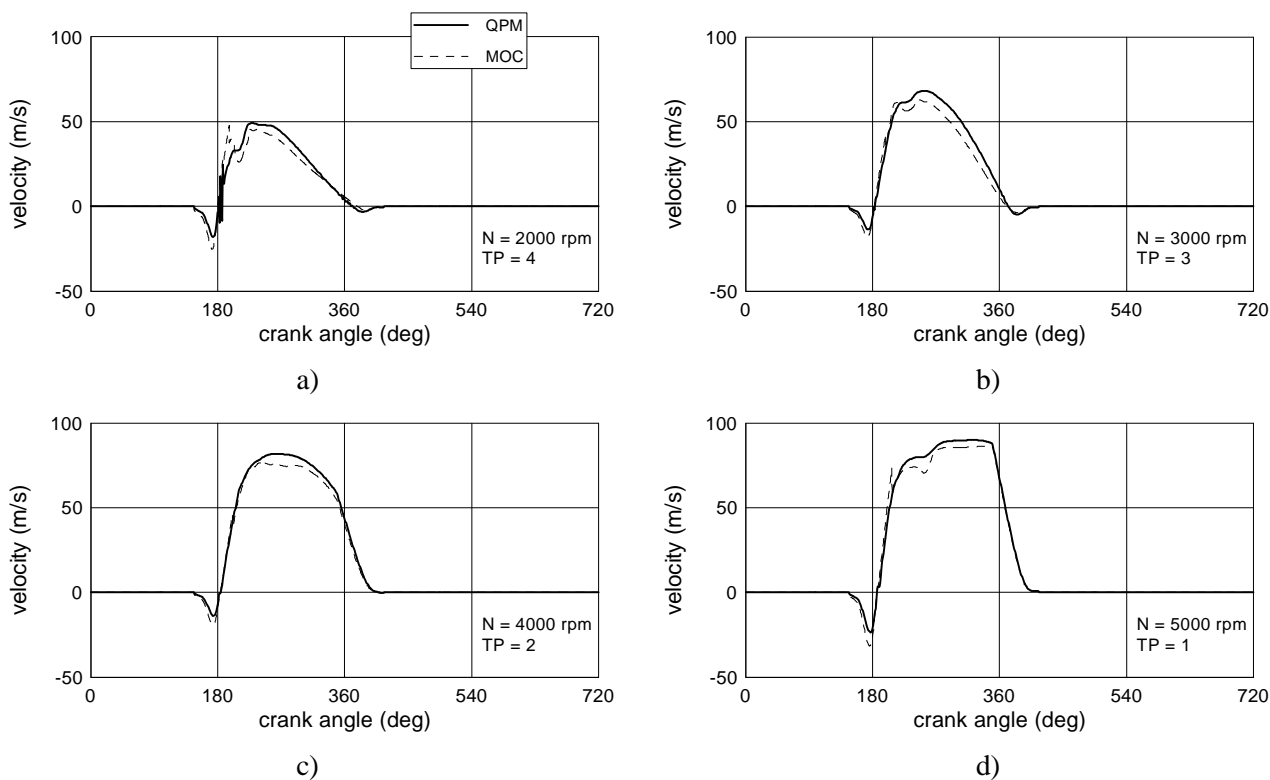


Figure 5: Fluid velocity in the intake pipe at different operating conditions (the crank angle has been set equal to zero at the BDC – end of the expansion stroke)

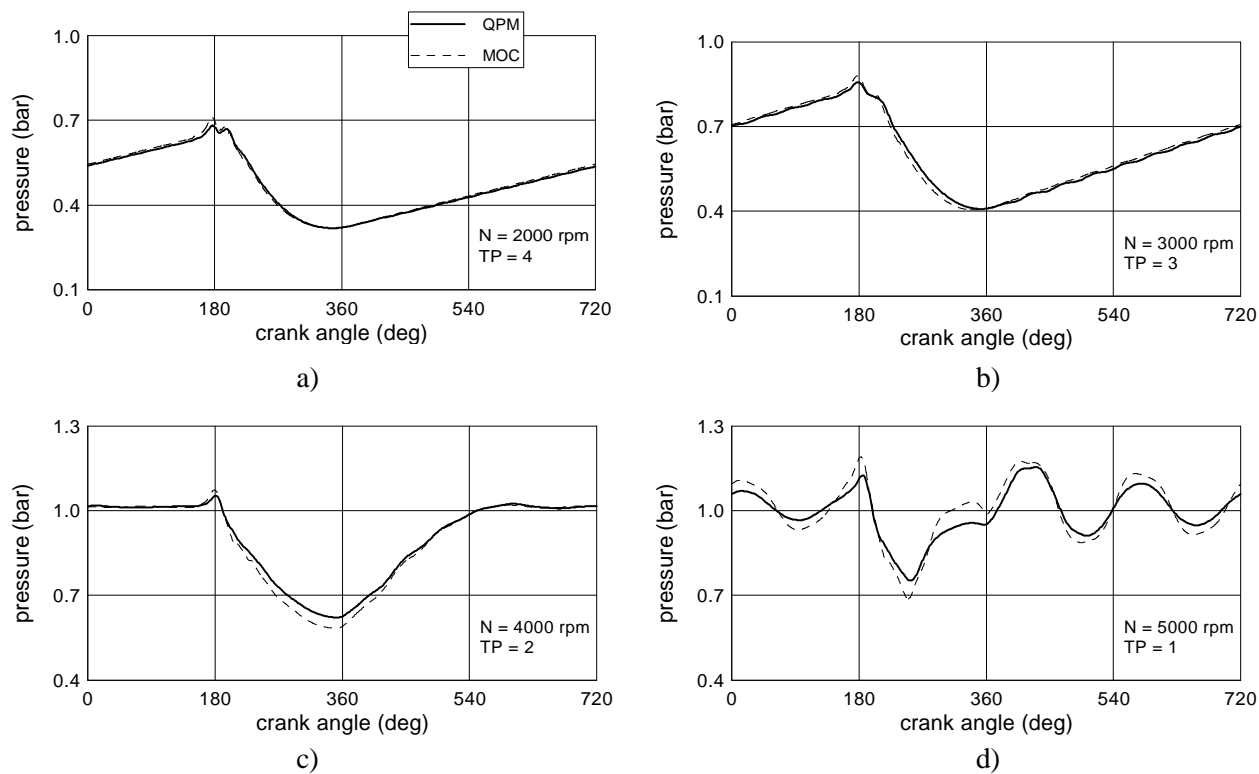


Figure 6: Fluid pressure in the intake pipe at different operating conditions

A more crucial test for the model validity derives from its application to the exhaust manifold, due to the presence of higher pressure differences with respect to the intake. In Figure 7, a comparison between the fluid velocity, at the midpoint of branch “10” (Figure 4) is presented. A quite satisfactory agreement between QPM and MOC is shown at low engine speed and load (Figure 7a); significant differences on the maximum and minimum fluid velocities can be observed at higher engine speed and load (Figure 7b). However, the prediction obtained with the QPM can be considered as appropriate for control purposes, being for these applications the mass trapped in the cylinder more relevant than the velocity and pressure values.

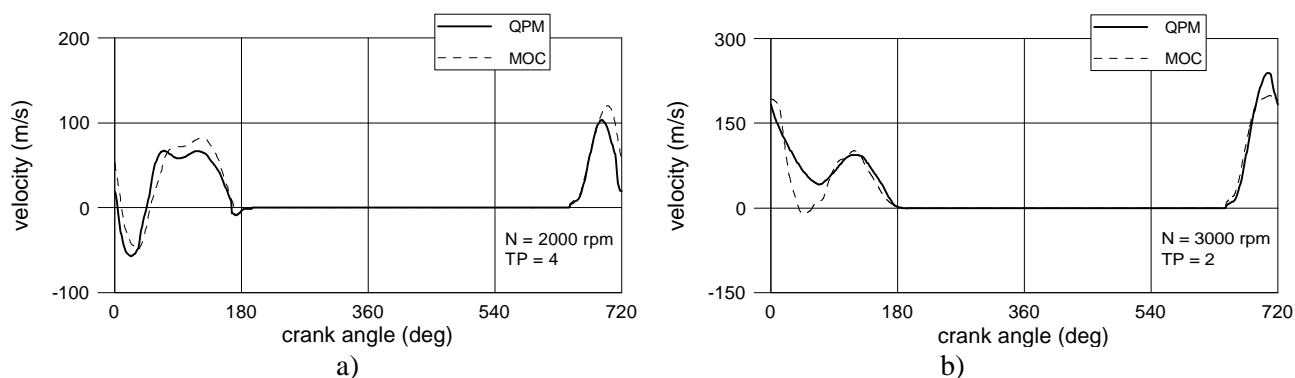


Figure 7: Fluid velocity in the exhaust pipe at different operating conditions

Figures 8a-b show, for steady engine operating conditions, the air mass maps as a function of the engine speed, the throttle valve position (Figure 8a) and the mean pressure just downstream the throttle valve (Figure 8b).

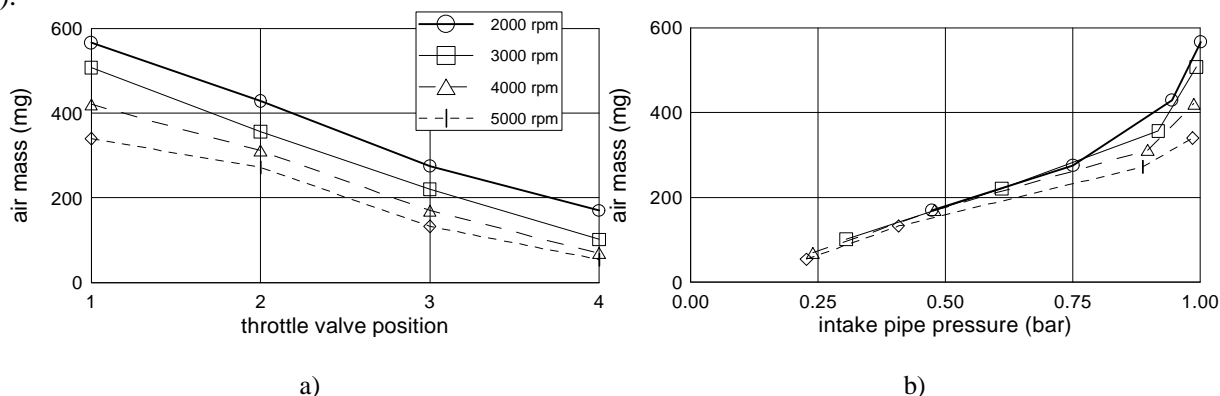


Figure 8: Engine steady maps

The first can be used in speed-throttle and the second in speed-density control strategies. The influence of the engine operating conditions on the volumetric efficiency, typical of a one-cylinder engine, is very well reported (an efficiency reduction of about 40% for TP=1 – WOT - and of about 70% for TP=4 results as the engine speed increases from 2000 to 5000 rpm).

### 3.2 Mixture formation, fuel dynamics and induction

The AFR inside the cylinder is strictly related to the air-fuel vapour mixture dynamics, as well as to the behaviour of the liquid fuel (droplets, puddles) in the intake port. Each contribution to the fuel inducted into the cylinder is characterized by a proper transfer time, resulting in a highly complex description of the overall fuel induction process. The present model, accounting for all the dynamics aspects in the port, allows for a

correct evaluation of the aforementioned time scales. In order to further analyze this aspect, the fuel injected has been evaluated, without any compensation (spray-wall interactions), from the air mass trapped into the cylinder calculated in the previous engine cycle; the characteristics of the engine under testing, moreover, cause that the fuel injection takes place completely with closed inlet valve, at all engine speeds.

Figures 9a-c illustrate the dynamics of the fuel mass in terms of vapour in the mixture and of film on the valve and on the port wall. This produces a complete characterization of the inducted fuel, being the fuel never inducted in form of drops, which are evaporated or impinged on the walls. The fastest transfer times are those related to the film on the valve (Figure 9a), which is suddenly and completely inducted in the early stage of the intake stroke, due to the high local fluid velocities. The fuel mass in vapour phase – mixture, Figure 9b – follows the air dynamics and therefore keeps the same induction times. The induction of the liquid fuel from the port wall is clearly much slower than the previous contributions (Figure 9c): this produces a fuel quantity stored in the puddle and never removed. These three contributions have transfer times which decrease as the engine speed increases: in all these cases, the air entrainment appears to be the dominant effect.

The behaviour of the port fuel puddle appears to be the most complex, due to the superposition of many phenomena that the model accounts for. Before IVO, at low engine speeds, the fuel mass decreases, due to evaporation and transfer to the fuel puddle on the valve. At higher engine speeds, the injection interval increases, producing an overall growth of the fuel mass on the port wall, due to the delay of the liquid drops arrival, which dominates on the effects of evaporation and transfer towards the valve. After IVC, the mass of the port wall film continues to decrease (almost with the same rate), due to the transfer in the valve puddle; after this phenomenon, the mass starts to increase due to the drops impingement.

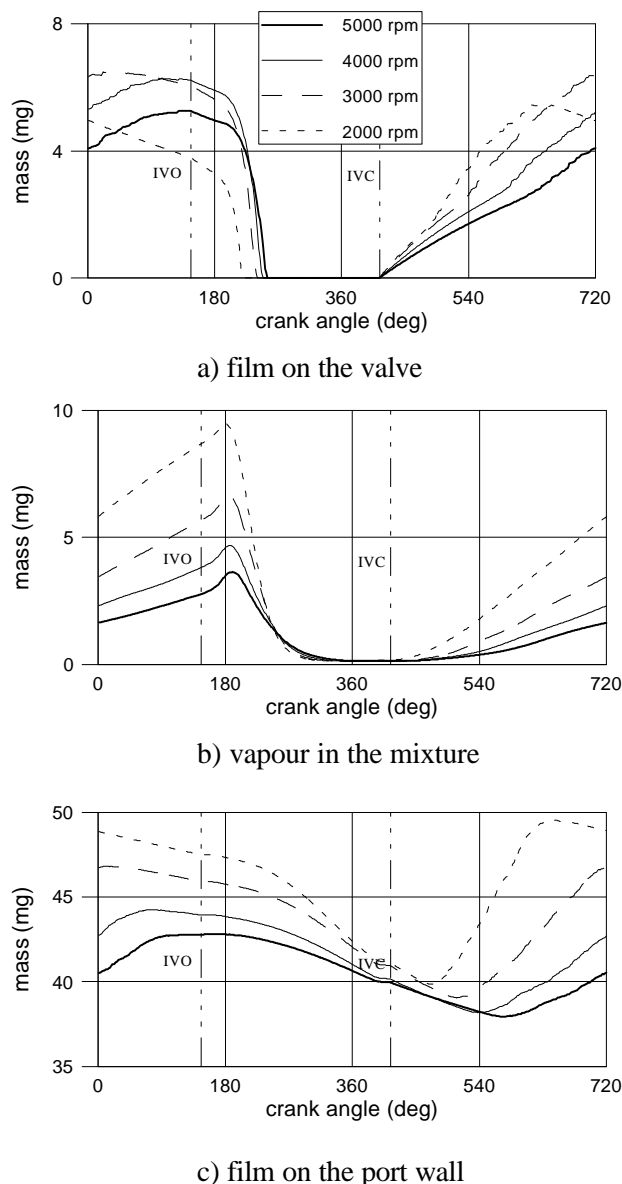


Figure 9: Time history of the fuel mass in the port (TP=1)

### 3.2 Transients and film compensation

The present model has been used in order to characterize the AFR excursions during typical engine transients and to evaluate the effectiveness of the well-known Aquino model (Aquino, 1981) to compensate these excursions. To examine the latter aspect, the two Aquino parameters  $X$  and  $\tau$  have been identified on the basis of the present model, by means of a step in the injected fuel flow rate. Processing the data of the injected and inducted fuel mass during the fuel transients at all engine speeds and loads, a table giving  $X$  and  $\tau$  values has

been obtained and stored in the model; this table has been used for evaluating the fuel compensation during engine transients.

Figure 10 illustrates the AFR excursions during a severe throttle transient. Figure 10a refers to an engine speed of 2000 rpm; Figure 10b to an engine speed of 5000 rpm. The dashed lines describe the effects of the fuel compensation, while the solid lines show the results of the model without it.

This compensation produces a stricter control of the AFR, more effective during throttle tip-in with respect to throttle tip-out. During this condition, the fuel appears over-compensated, leading to a lean mixture following the rich mixture period due to the throttle valve closing. Moreover, the transient dynamics of the fuel vapour entrained by the air is neglected by the Aquino model and therefore uncompensated.

In absolute terms, the AFR excursions appear underestimated with respect to the real case: in fact, the fuel injected is calculated according to the trapped air evaluated by the model at the previous cycle. Real on-board sensors have their own response time; besides, they do not account for the air unsteadiness between the measurement section and the inlet valve.

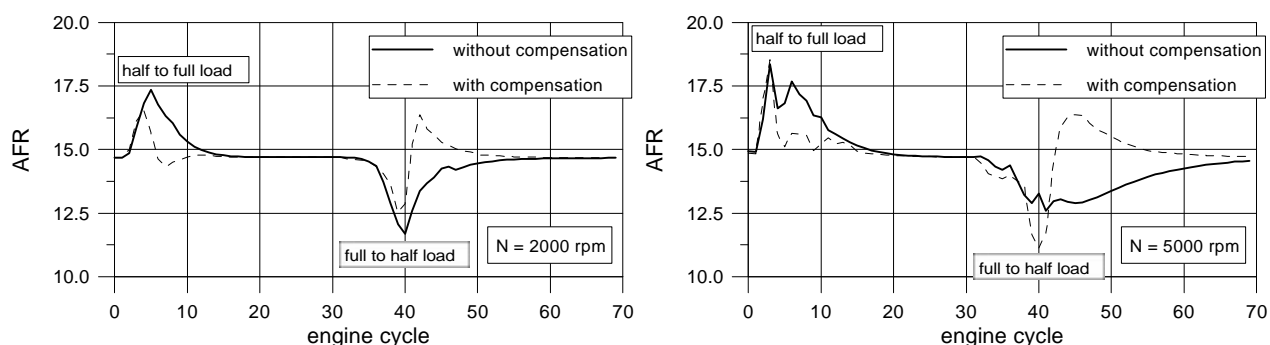


Figure 10: AFR during engine transients

## 4 Conclusions

In this paper a comprehensive model of ICE oriented to the electronic control of the injection is presented. A key role in this model is played by the coupling of a Quasi Propagatory Model for the air and the exhaust gas dynamics with a model of the fuel dynamics that makes use of a quasi-lagrangian approach.

Due to the first model, real intake and exhaust configurations can be accounted for (filters, mufflers, collectors, runners, catalyts, etc.) considering the unsteadiness due to pressure waves propagation; the second model considers droplets motion, fuel puddles on the port wall and on the valve, fuel evaporation due to heat transfer and molecular diffusion.

The overall model allows for:

1. an on-board application for fuel injection control, if further simplified on the fuel dynamics description;
2. an out-of-board application for the evaluation of the air maps, according to the requirements of speed-throttle, speed-density and MAF control strategies;
3. an identification of the constants in the Aquino model, widely used for the fuel compensation during engine transients.

The model has been used as a predictive tool of the AFR excursions during transients of engines equipped with the widespread adopted Aquino fuel compensation strategy.

The fuel dynamics in vapour phase associated with the air entrainment, though neglected in practical applications, has shown a great importance.

## Acknowledgements

This work was supported by the Research Fund "MURST 40%" and by the "Consiglio Nazionale delle Ricerche" under the Research Project "Sviluppo di metodologie teorico-sperimentali per lo studio e la progettazione di sistemi di controllo elettronico per motori ad accensione comandata".

## References

- Aquino, C.F. (1981). "Transient A/F control characteristics of the 5 liter central fuel injection engine," *SAE Paper 810494*.
- Anatone, M., Cipollone, R., Milazzo, A. (1998a). "A model for mixture formation in port injected SI engines," *2nd International Conference on Control and Diagnostics in Automotive Applications*, Genova, Italy, October 1998, no. 98A5047.
- Anatone, M., Carapellucci R., Milazzo, A. (1998b). "Analisi mediante diffrazione laser del getto di un iniettore per MCI ad accensione comandata," *53rd Congresso Nazionale ATI*, Firenze, Italy, September 1998.
- Cipollone, R., Sciarretta, A. (1998a). "On the air dynamics in ICE intake manifolds. The development of a quasi propagatory model," *6th IEEE Mediterranean Conference on Control and Systems*, Alghero, Italy, June 1998.
- Cipollone, R., Sciarretta, A. (1998b). "On the modelling of the gas dynamics in spark ignition ICE manifolds oriented to A/F control," *2nd International Conference on Control and Diagnostics in Automotive Applications*, Genova, Italy, October 1998, no. 98A5048.
- Cipollone, R., Sciarretta, A. (1998c). "Un contributo sulla previsione del rapporto aria-combustibile nei MCI ad accensione comandata," *53th Congresso Nazionale ATI*, Firenze, Italy, September 1998.
- Hendricks, E. (1996). "Engine modelling for control applications: a critical survey," *1st International Conference on Control and Diagnostics in Automotive Applications*, Genova, Italy, October 1996, no. 96A4009.
- Heywood, J. (1988). *Internal combustion engine fundamentals*, McGraw-Hill, 1998.
- Horlock, J., Winterbone, D. (1986). *The thermodynamics and gas dynamics of internal-combustion engines*, vol. 2. Clarendon Press, Oxford, 1986.
- Maki, H., Akazaki, S., Hasegawa, Y., Komoriya, I., Nishimura, Y., Hirota, T. (1995). "Real time engine control using STR in feedback system," *SAE Paper 950007*.
- Nasu, M., Ohata, A., Abe, S. (1996). "Model-based fuel injection control system for SI engines," *SAE Paper 961188*.
- Ohata, A., Ohashi, M., Nasu, M., Inoue, T. (1995). "Model based air fuel ratio control for reducing exhaust gas emissions," *SAE Paper 950075*.
- Toyota Engine Technology* (1996). Chapter 5, Toyota motor corporation, Aichi, Japan.
- Weeks, R., Moskwa, J. (1995). "Automotive engine modeling for real-time control using MATLAB/SIMULINK," *SAE Paper 950417*.